J. Fluid Mech. (1985), *vol.* 150, *pp.* 89–119
Printed in Great Britain

Natural convection in porous media

By V. PRASAD,
Department of Mechanical Engineering, Columbia University, New York, NY 10027

F. A. KULACKI AND M. KEYHANI
Department of Mechanical and Aerospace Engineering, University of Delaware, Newark, DE 19716

(Received 8 March 1984)

Experimental results on free convection in a vertical annulus filled with a saturated porous medium are reported for height-to-gap ratios of 1.46, 1 and 0.545, and radius ratio of 5.338. In these experiments, the inner and outer walls are maintained at constant temperatures. The use of several fluid–solid combinations indicates a divergence in the Nusselt-number–Rayleigh-number relation, as also reported by previous investigators for horizontal layers and vertical cavities. The reason for this divergence is the use of the stagnant thermal conductivity of the fluid-filled solid matrix. A simple model is presented to obtain an effective thermal conductivity as a function of the convective state, and thereby eliminate the aforementioned divergence. A reasonable agreement between experimentally and theoretically determined Nusselt numbers is then achieved for the present and previous experimental results. It is thus concluded that a unique relationship exists between the Nusselt and Rayleigh numbers unless Darcy's law is inapplicable. The factors that influence the breakdown of Darcian behaviour are characterized and their effects on heat-transfer rates are explained. It is observed that, once the relation between the Nusselt and Rayleigh numbers branches out from that obtained via the mathematical formulation based on Darcy's law, its slope approaches that for a fluid-filled enclosure of the same geometry when the Rayleigh number is large enough. An iterative scheme is also presented for estimation of effective thermal conductivity of a saturated porous medium by using the existing results for overall heat transfer.

1. Introduction

Fundamental investigations of natural convection in saturated porous media appear to have started with linearized stability theory applied to an infinite horizontal layer heated from below (Horton & Rogers 1945; Lapwood 1948). These studies established the criterion for the onset of convection which was experimentally verified by various other investigators later on. Soon thereafter, both analytical and experimental investigations were conducted to determine convective heat-transfer rates through saturated permeable media of various geometric shapes, e.g. rectangular cavities and horizontal and vertical annuli. Some of these studies were aimed at visualizing the flow field and the temperature distributions as well. Extensive reviews of prior work have been presented by Combarnous & Bories (1975) and Cheng (1978). Generally, prior studies have considered constant-temperature boundaries, and only recently have studies begun to appear in which constant-flux boundaries were considered (e.g. Prasad & Kulacki 1982; Kulkarni 1983; Reda 1983).

Most analytical and numerical studies of natural convection in porous media are

based on the formulation presented by Wooding (1957). For an isotropic, homogeneous fluid-saturated porous media obeying Darcy's law, the equations for conservation of mass and momentum under steady-state conditions are

$$\nabla\cdot(\rho \boldsymbol{V}) = 0, \tag{1}$$

$$\frac{\rho}{\epsilon^2}(\boldsymbol{V}\cdot\nabla)\,\boldsymbol{V} = -\nabla p + \rho \boldsymbol{g} - \frac{\mu}{K}\boldsymbol{V}, \tag{2}$$

where ϵ and K are respectively the porosity and permeability of the porous medium, ρ and μ are the density and dynamic viscosity of the fluid, and p is the pressure. The velocity vector $\boldsymbol{V}$ is given as $\boldsymbol{V} = \epsilon \boldsymbol{q}$, where $\boldsymbol{q}$ is the fluid-particle velocity vector.

Neglecting the viscous dissipation, the energy equation obtained by Wooding (1957) is

$$\rho C(\boldsymbol{V}\cdot\nabla T) = \nabla\cdot(k\,\nabla T), \tag{3}$$

where C is the isobaric specific heat of the fluid and k is the effective thermal conductivity of the porous medium. For an isotropic homogeneous medium this equation can be written as

$$\boldsymbol{V}\cdot\nabla T = \alpha\nabla^2 T, \tag{4}$$

where α is the thermal diffusivity $k/\rho C$ of the fluid-saturated porous medium.

A vast majority of the analytical and numerical results available are based on the solution of (1), (2) and (4) with the Boussinesq approximation of linear density variation. In most of these analyses, the inertia term in (2) has been neglected owing to its low order of magnitude. Non-dimensionalization of these equations under the above conditions leads to a modified Rayleigh number

$$Ra^* = \frac{\rho g \beta K D\,\Delta T}{\mu\alpha} = Ra_f\, Da \frac{k_f}{k}, \tag{5}$$

where ΔT is the temperature difference across the porous layer, D is a characteristic length (e.g. gap width), β is the isobaric coefficient of thermal expansion for the fluid, k_f is the fluid thermal conductivity, Ra_f is the fluid Rayleigh number and $Da = K/D^2$ is the Darcy number. Depending on the shape of enclosure, some geometric parameters are also obtained, such as the aspect ratio $A = L/D$ (height to gap width) in rectangular enclosures, or the radius ratio $\kappa = r_o/r_i$ (outer/inner radii) and the aspect ratio A for the annular enclosures. The Prandtl number $Pr^* = C\mu/k$ of the medium does not appear explicitly in the mathematical formulation, once the convective terms in (2) are dropped.

Efforts have also been made to include the viscous diffusion term as $\mu'\nabla^2\boldsymbol{V}$ in the momentum equation as proposed by Brinkman (1949). When $\mu' = \mu$ this term leads to the Darcy number, which is usually very small. Results obtained by using the Brinkman model such as those by Chan, Ivey & Barry (1970) clearly indicate that the contribution of this additional viscous term in the momentum equation is almost negligible for any reasonable value of Da. Hence most of the analytical and numerical results have been presented only in terms of the Rayleigh number and the geometric parameters. These results clearly indicate that the properties of the solid and fluid and the structure of the porous medium affect the heat transfer and flow behaviour only through the Rayleigh number Ra^*.

Compared with existing analytical work, experimental investigations are very limited. Some of the important experimental results are due to Schneider (1963), Elder (1967), Katto & Masuoka (1967), Combarnous (1970*a*, *b*), Kaneko, Mohtadi & Aziz (1974), Buretta (1972) and Yen (1974) for horizontal layers, to Bories & Combarnous (1973) and Kaneko *et al.* (1974) for inclined layers, to Schneider (1963),

Klarsfeld (1970), Bories & Combarnous (1973) and Seki, Fukusako & Inaba (1978) for vertical cavities, and to Reda (1983), Kulkarni (1983) and Prasad & Kulacki (1984*b*) for vertical annuli. Out of these, most of the experiments have been conducted for a porous medium comprising randomly packed glass beads and water as the saturating fluid.

The data obtained by using various combinations of solid particles and fluids (Schneider 1963; Combarnous 1970*a*, *b*; Seki *et al.* 1978) are quite interesting and reveal that the heat-transfer rate is not only a function of the Rayleigh number but also depends on the properties of the medium. This is contrary to what the mathematical formulation indicates. For example, for a vertical rectangular cavity of $A = 7.5$, Schneider (1963) reports a Nusselt number for a glass–water medium to be 2.3 times larger than that for a steel–turpentine medium when $Ra_{\mathrm{m}}^{*} = 600$. (The subscript m denotes the use of stagnant thermal conductivity k_{m} for the medium.) The results of Combarnous (1970*a*, *b*) and Seki *et al.* (1978) show a similar behaviour. A summary of the various experimental and analytical results for a horizontal layer heated from below has recently been given by Cheng (1978). His summary plot of the average Nusselt number versus the Rayleigh number is an excellent indication of large-scale divergence between the heat-transfer results. From this plot one can observe that the heat-transfer coefficients reported by Elder (1967) for a glass–water medium is up to five times higher than that for the steel–turpentine medium given by Schneider at specific values of Rayleigh number.

Various theories have been proposed to explain this divergence in the heat-transfer results. Schneider (1963) has argued that, as the convective effects increase with an increase in Ra_{m}^{*}, the influence of thermal conductivity k_{m} of the layer decreases while that of the thermal conductivity k_{f} of the fluid increases. (Note that all the reported experimental results are based on k_{m}.) To show a better agreement in heat-transfer results for various media, he presented his experimental results in terms of Rayleigh and Nusselt numbers based on the fluid conductivity k_{f}. Though the agreement among the results for various media improved at high Rayleigh numbers, the heat-transfer results diverged at low values of $Gr^{*}Pr_{\mathrm{f}}$ owing to this scaling, where $Gr^{*} = \rho^{2} g \beta K D \Delta T / \mu^{2}$. Combarnous (1972) has attributed the cause of this divergence to the invalid assumption of an infinite heat-transfer coefficient between the fluid and solid phases. He has proposed an analytical model based on two energy equations, one for the solid phase and the other for the liquid phase. His model involves two more dimensionless parameters other than Ra_{m}^{*} and A for a horizontal layer. The numerical results obtained by Combarnous & Bories (1974) by using this model indicate that there were still appreciable differences between the analytical and experimental results, as large as up to 42 %. Secondly, to obtain any satisfactory result from this model, one needs to know reasonable values for the thermal conductivity k_{s}^{*} of the dispersed structure of the solid matrix, the conductivity k_{f}^{*} of the fluid which includes the effects of hydrodynamic dispersion, and the volumetric heat-transfer coefficient h_{p} between the solid and liquid phases.

Other investigators believe that this divergence is a result of a Prandtl-number effect, other than that included in Ra_{m}^{*}. Based on the experimental results for a vertical cavity, Seki *et al.* (1978) have concluded that Pr_{m}^{*} has an exponent of 0.13 when the Nusselt number is correlated by an equation of the form

$$Nu_{\mathrm{m}} = \text{constant} \times Ra_{\mathrm{m}}^{*r} Pr_{\mathrm{m}}^{*s}, \tag{6}$$

where r and s are experimentally determined constants. Seki *et al.* have used different combinations of glass and iron balls and water, alcohol and transformer oil to produce

the saturated porous medium. Recently, Catton (1984) has also reported a correlation of the form of (6) for a horizontal layer. The value of s obtained by him is 0.18 for $0.5 < Pr_m^* < 11$.

Another interesting feature of these experimental results is the change in the slope of $\ln Nu_m$ when plotted versus $\ln Ra_m^*$ at higher values of the Rayleigh number. The Rayleigh number at which the decrease in slope starts appears to depend on the mean diameter of the solid particles. Also, the results of Schneider (1963), Combarnous (1970*a*, *b*), Buretta & Berman (1976), Seki *et al.* (1978) and others indicate that, for the same solid–fluid combination, the heat-transfer rate is a function of particle size. Larger mean particle diameters tend to produce a lower Nusselt number when $k_f < k_s$ and an earlier transition to a lower slope on the $\ln Nu_m$ versus $\ln Ra_m^*$ curve.

2. Motivation and objectives of the present study

As mentioned earlier, analytical and numerical results have been reported for various types of enclosures filled with saturated porous media. Out of these a substantial amount of work has been done on the rectangular cavity particularly when either the vertical or the horizontal walls are maintained at constant temperatures with the other walls insulated. A review of the studies made on the rectangular cavity with isothermally heated vertical wall has recently been presented by Prasad (1983). The effects of curvature on an isothermally heated vertical enclosure has also been recently studied by Hickox & Gartling (1982), Havstad & Burns (1982), Prasad (1983) and Prasad & Kulacki (1984*a*, *b*). In all of these studies, a vertical annulus with an isothermal inner wall has been considered. The outer wall has been assumed as isothermally cooled and the top and bottom walls are insulated. Havstad & Burns have also considered the effect of a conducting outer wall. Experimental results have also been reported for the annulus heated by uniform heat flux on the inner wall (Reda 1983; Kulkarni 1983).

Using finite-element technique and an approximate method, Hickox & Gartling have obtained heat-transfer results for tall annuli ($A \geqslant 2$) and low Rayleigh numbers Ra^* up to 100. Using three different methods (finite-difference, approximate and perturbation), Havstad & Burns have presented results for $1 < \kappa < 10$, $0.5 \leqslant A(\kappa-1)/\kappa \leqslant 20$ and $35 \leqslant Ra^*\kappa/(\kappa-1) \leqslant 150$, where $\kappa = r_o/r_i$ is the radius ratio and $A = L/D$ is the aspect ratio (height to annular gap width). Prasad & Kulacki (1984*a*, *b*) have considered the problem for much wider ranges of radius ratio and Rayleigh numbers, i.e. $1 \leqslant \kappa \leqslant 26$ and Ra^* up to 10000. Using a finite-difference numerical scheme they have studied the curvature effects on temperature and flow fields, and the heat-transfer rates for $1 \leqslant A \leqslant 20$ in the first paper (1984*a*) and for $0.3 \leqslant A \leqslant 1$ in the second paper (1984*b*).

Recently, the first experimental studies of natural convection in a vertical annulus have been reported by Reda (1983) and Prasad & Kulacki (1984*b*). Reda's work involved the use of a constant heat flux on the inner cylinder and an isothermal outer cylinder. Owing to the application of his work to the technology of nuclear waste disposal, a permeable medium of 320 ± 75 μm diameter (i.e. 50-mesh) particles and an overlying constant-pressure fluid layer were used. The major results were that the inner-surface temperature increased with distance from the bottom of the annulus, even at relatively low Rayleigh numbers of 10 or less, and that the temperature distribution across the gap was progressively below that for conduction as the power input to the inner cylinder was increased. Reda did not present a correlation for Nusselt number versus Rayleigh number owing to the small range of Rayleigh

numbers considered. Also, he used a relatively large radius ratio, $\kappa = 23$ with $A = 4.25$, owing to a focus on temperature distributions in his measurements. Prasad & Kulacki (1984*b*) have used glass beads of 3 mm and 6 mm diameter with water as the working fluid to conduct their experiments for an isothermally heated annulus with $A = 1$ and $\kappa = 5.338$. They have reported close agreement between numerically and experimentally determined values of Nusselt number for $Ra_m^* \leqslant 4000$. Experimental temperature distributions are also reported to be in reasonably good agreement with numerical predictions.

Based on our review of the current literature, it is evident that few reports are available on natural convection in vertical annuli filled with saturated porous media, and, of these, experimental studies are rare. Also, experimental work that is available, regardless of geometry, is generally limited with respect to solid–fluid combinations. To our knowledge, only Schneider (1963), Combarnous (1970*a*, *b*), Kaneko *et al.* (1974) and Seki *et al.* (1978) have conducted experiments using various combinations of solid particles and fluids. Thirdly, the divergence in the heat-transfer results as discussed above has not been properly explained, nor has the breakdown of classical Darcian assumptions at high Rayleigh number been characterized and explained as well.

The objectives of the present experimental study are hence multifold. They are: (1) to obtain the heat-transfer results and the temperature distributions for the isothermally heated vertical annuli for various combinations of fluid and solid to produce the porous media and compare them with the numerical predictions; (2) to characterize the Prandtl-number effect on the natural convection in porous media; (3) to explain the divergence in the heat-transfer results depending on the solid–fluid combinations; (4) to characterize the breakdown of Darcy's behaviour for natural convection in the enclosures filled with porous media; (5) to investigate the heat-transfer behaviour of porous media once Darcy's law has become inapplicable.

In order to achieve the above objectives, the experiments have been conducted for a vertical annulus whose inner and outer walls are isothermal, the top and bottom being insulated. Glass and steel beads of various sizes have been used as solids, while water, heptane and ethylene glycol have been used as saturating fluids. For the present experiments, the radius ratio of the annulus is 5.338, while the aspect ratio has been varied to obtain results for $A = 1.46$, 1 and 0.545. These results are then carefully analysed to explain the divergent behaviour of the heat-transfer results.

3. Experimental apparatus and procedure

A schematic of the experimental apparatus used for the present experiments is given in figure 1. The inner cylinder is made out of a wood rod, a glass–epoxy cylinder and a brass cylinder. To obtain a constant-temperature inner surface, eight thermofoil heaters of 31.8 mm width and 160 mm long are wrapped around the glass–epoxy cylinder, which is then inserted into a brass cylinder of 57.1 mm outer diameter. A wood rod is shrink-fitted into the glass–epoxy cylinder. To monitor the temperature at various locations on the inner-cylinder surface, 15 thermocouples are embedded in the wall by making slots of 2.5 mm depth in the brass cylinder. The slots are then covered with copper cement and sanded to have smooth inner surface. This type of arrangement is preferred because the thermocouples attached to the wall disturbs the flow field and indicates a temperature between that of the wall surface and the exposed surface.

A brass cylinder of 304.8 mm inner diameter and 5.1 mm thick is used as the outer cylinder, and is maintained at a constant temperature by circulating water at a

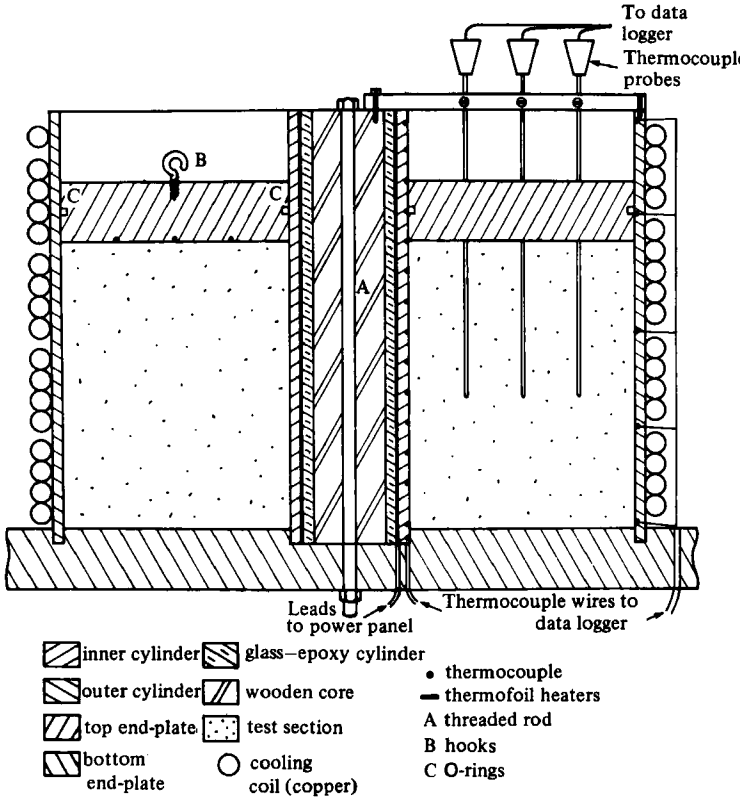

FIGURE 1. Schematic of experimental apparatus.

constant temperature through a copper tube wrapped and soldered around it. Five thermocouples are embedded into the wall at 0.25 mm away from the inner surface. For the base plate and the top cover, a 31.75 mm thick Phenolite ($k = 0.293$ W m^{-1} °C^{-1}) sheet is used. The top cover plate is provided with two O-rings, one each on the outer and inner side walls, and is free to move up and down. This facilitates in obtaining data for three different aspect ratios, $A = 1.46$, 1 and 0.545, by changing the height of the medium. Three thermocouples are cemented to its inner surface at radially equidistant locations, as shown in figure 1. Three copper–constantan grounded thermocouple probes (3.2 mm diameter) are used to measure the temperature inside the medium.

To provide and control the power in each heater a power panel with an independent circuit for each heater is used. The thermocouple readings are directly taken in degrees Celsius by using a datalogger, which is able to read temperatures to the first decimal place. A constant-temperature circulator is used to circulate cooling water maintained to ± 0.1 °C through the copper coil. A detailed account of the experimental arrangement is presented by Prasad (1983).

To obtain a saturated porous medium, the annular gap is filled up to the required height with solid balls and the saturating liquid, pouring them one by one. The balls are allowed to settle down in a random manner by stirring them continuously. Finally, liquid is added in excess and the top plate is placed and pushed to the position where it rested on the balls, allowing the excess liquid to come out.

The height of the working medium is always kept approximately equal to an integer multiple of the heater width. Power is supplied to two additional heaters, one at the

Aspect ratio A	Liquid	Solid	Ball diameter d (mm)	Rayleigh number Ra_m^*	Percent maximum temperature variation on surface: inner	Percent maximum temperature variation on surface: outer
1.46	ethylene glycol	glass	3	12–163	0.14	0.88
	water	glass	6	160–4578	0.32	5.29
1.00	water	glass	22.25	1804–167419	0.42	2.19
	heptane	glass	3	215–1357	1.96	2.07
	heptane	glass	6	558–3808	1.51	0.88
	ethylene glycol	glass	3	27–130	0.20	0.43
	ethylene glycol	glass	6	26–589	0.39	1.59
	water	chrome steel	6.35	44–521	3.20	2.60
0.545	water	glass	3	66–1040	0.70	1.55
	water	glass	6	103–8430	1.87	3.70
	heptane	glass	3	166–1726	1.69	0.43
	heptane	glass	6	1439–7832	3.00	1.63
	ethylene glycol	glass	3	39–192	0.56	0.45
	ethylene glycol	glass	6	75–691	0.53	0.47
	water	chrome steel	6.35	74–400	0.67	0.50

TABLE 1. Experimental range of aspect ratio, Rayleigh number and solid–fluid combinations for radius ratio $\kappa = 5.338$ for the present experiments

bottom end and one in parallel with the top cover plate. These heaters help to minimize conduction losses. Every 2–3 h, the temperature distribution on the inner surface is checked to make sure that it is being maintained at a constant temperature. Manual adjustment of power input to each heater is then done if needed. In general, 10–30 h are required to reach the desired steady state and make one set of readings. The maximum temperature variations on the inner and outer walls of the annulus are given in table 1.

Temperature corrections are applied to the thermocouple readings to account for the distances by which they are away from the inner and outer surfaces. To estimate the conduction loss through the top plate, temperatures at five locations on the upper surface of the plate are recorded with the help of a digital thermometer. The conduction loss through the bottom end plate is very small, less than 0.5 % of the power input (Prasad 1983), and is neglected in calculating the net power input. The fact that this loss is negligible, is also evident from the numerical results (Prasad & Kulacki 1984*a*), which indicate the presence of a thick cold layer in the lower region of the annulus.

By using a measured amount (mass) of solid beads to fill the annulus to the required height, the porosity ϵ of the medium is obtained by calculating the volume of the solid beads and the total volume. The permeability of the porous medium is then calculated by using the Kozeny–Carman equation (Bear 1972)

$$K = \frac{d^2}{180}\frac{\epsilon^3}{(1-\epsilon)^2}, \tag{7}$$

where d is the average diameter of the solid beads.

The stagnant thermal conductivity k_m of the porous medium is obtained using the correlation of Kunii & Smith (1960). This correlation is based on the theoretical equations for predicting the stagnant conductivities in packed beds of unconsolidated particles. Yagi, Kunii & Wakao (1961) have compared the theoretical predictions for k_m with the experimental values of radially effective thermal conductivities for various porous media, a geometric configuration very close to the present one. The agreement has been reported to be reasonably good. Experimental values of k_m obtained by Katto & Masuoka (1967) for horizontal porous layer also agree well with the empirical predictions by using Kunii & Smith's correlation. Furthermore, the agreement between theoretical values of conduction Nusselt number and experimental results at very low Rayleigh numbers in the present experiments and those conducted by Kulkarni (1983) indicates that the correlation predicts reasonably good values of stagnant thermal conductivity, at least for the radial-heat-transfer case.

The average heat-transfer coefficient on the inner vertical wall is calculated as

$$\bar{h} = \frac{\text{net power}}{(\text{inner-surface area}) \times (\text{temperature difference})}. \tag{8}$$

The Nusselt number is then obtained as $Nu_m = \bar{h}D/k_m$.

4. Results

For $\kappa = 5.338$ and $A = 1.46$, 1 and 0.545 experiments were conducted for a wide range of Rayleigh number as given in table 1. To obtain data for various fluid–solid combinations, glass beads of 3, 6 and 22.25 mm diameter, and chrome-steel beads of 6.35 mm diameter were used with water, heptane and ethylene glycol. This covered a range of effective Prandtl number Pr_m^* from 0.5 to 100.

To make direct comparison between the present experimental results and the theoretical predictions, numerical computations were carried out for the present values of κ and A by employing a finite-difference method used by Prasad & Kulacki (1982, 1983, 1984*a*, *b*). The method and its computational aspects have already been presented elsewhere (Prasad & Kulacki 1982, 1984*a*) and will not be discussed here. It may be noted that these numerical solutions are based on Wooding's formulation of the problem and use (1)–(3), without the inertia term in (2). While presenting the experimental results, numerical predictions have also been plotted wherever possible. For experimental results, the Rayleigh and Nusselt numbers are either based on the stagnant thermal conductivity k_m or the effective thermal conductivity k_e (to be discussed later). For comparison and analysis of data for various porous media, the experimental results for water–glass (3 and 6 mm diameter beads, $A = 1$) have been reproduced from Prasad & Kulacki (1984*b*).

4.1. *Temperature distributions*

Temperature in the r-direction was recorded at five different heights $z/L = 0$, 0.25, 0.50, 0.75 and 1 in order to examine the behaviour of heat transfer through the annular porous layer. Figures 2–4 present the typical non-dimensional temperatures θ at three radial locations $R = 0.25$, 0.50 and 0.75, where $\theta = (T-T_0)/(T_i-T_0)$ and $R = (r-r_i)/(r_o-r_i)$. (More temperature distributions are presented by Prasad 1983.) In these figures the experimentally obtained values of θ are plotted along with the theoretical temperature distributions at those heights. Figure 2(*a*) presents the temperature distributions for $Ra_m^* = 100$ and $A = 1.46$ for a glycol–glass medium with $d = 3$ mm. The agreement between the numerical predictions and the recorded

temperature is excellent. The largest difference between the two is about 8 %. Similar agreement is also observed for $Ra_m^* = 1000$, except for $Z = z/L \leqslant 0.25$ (figure 2*b*). Also, measured temperatures in the upper region are higher than the numerical values. This difference increases at larger Rayleigh numbers. At $Ra_m^* = 5000$ the measured temperatures are about 30 % higher than predicted values at $Z = 0.75$ (figure 2*c*). The agreement in the lower region of the annulus, $Z \leqslant 0.5$, is quite reasonable.

In figures 3 (*a–c*) the temperatures for various porous media are presented for $A = 1$. The agreement between the numerical and experimental values of θ for water–glass ($d = 3$ mm and 6 mm) is quite reasonable as already reported (Prasad & Kulacki 1984*b*). The maximum difference between the two values is 16.5 % at $Ra_m^* = 2000$. Again, the actual temperatures in the upper region of the porous medium, $Z > 0.5$, are higher than predicted values for high values of Rayleigh number (figure 3*c*).

As can be seen, the temperature at any location in the medium depends on the solid–fluid combination. For $Ra_m^* \approx 200$ temperatures for water–steel at $Z \leqslant 0.75$ are all lower than that for water–glass, and temperatures for glycol–glass are mostly higher than that for the water–glass at the same locations (figure 3*a*). For $Z > 0.75$ the temperatures for water–steel are not only higher than those for the water–glass, but are also higher than the numerical predictions. For lower values of Rayleigh number, this difference between the values of θ for water–steel and other media at $Z = 1$ is much larger (Prasad 1983). As Ra_m^* increases, the temperatures for water–steel at $Z = 1$ decrease further, and at $Ra_m^* \approx 500$ they are lower than all the numerical and experimental values of θ except for heptane–glass (figure 3*b*).

It is further observed that the temperatures for glycol–glass and heptane–glass are mostly higher than that for water–glass when $Z \leqslant 0.75$ (figures 3*a–c*). At $Z = 1$ the behaviour is completely different. There the temperatures for glycol–glass and heptane–glass are both lower than those for water–glass.

Temperatures for $A = 0.545$ are presented in figures 4 (*a–c*). The behaviour of recorded temperatures for various porous media is almost the same as discussed earlier. Again, in the present case the temperatures for water–steel are lower than the numerical predictions for $Z \leqslant 0.75$, whereas in the upper region they are higher than the numerical values. This difference between the experimental and numerical values decreases as the Rayleigh number increases (figures 4*a*, *b*, also Prasad 1983). Furthermore, in the lower region ($Z \leqslant 0.75$), temperatures for glycol–glass are higher than those for water–steel (figure 4*b*), but the behaviour reverses as $Z \rightarrow 1$. From figure 4 (*c*) it can be observed that for $Z \leqslant 0.75$ the values of θ for heptane–glass are higher than those for glycol–glass, whereas, at $Z = 1$, the reverse is true.

This behaviour of the temperature distributions can be summarized as follows.

(*a*) For glass as the solid medium the temperatures for heptane are in general higher than that for the glycol, which in turn are higher than that for water, when $Z \leqslant 0.75$. Since the thermal conductivity for the heptane is lowest and that for the glycol lies between the heptane and the water, the implication is that for a given k_s, the temperatures for a porous medium with small k_f/k_s are higher than those for a medium with larger k_f/k_s ($Z \leqslant 0.75$). When $Z \rightarrow 1$ this behaviour is reversed. (The subscripts f and s denote fluid and solid respectively.)

(*b*) For water as the saturating fluid, the temperatures for the glass are higher than those for the steel, when $Z \leqslant 0.75$. This implies that for a given value of k_f, a larger k_s/k_f produces lower temperatures for Z less than a certain value, whereas above this value the reverse is true. As the fluid velocity increases, the difference in the lower region diminishes, and in the upper region the behaviour is just reversed. This is

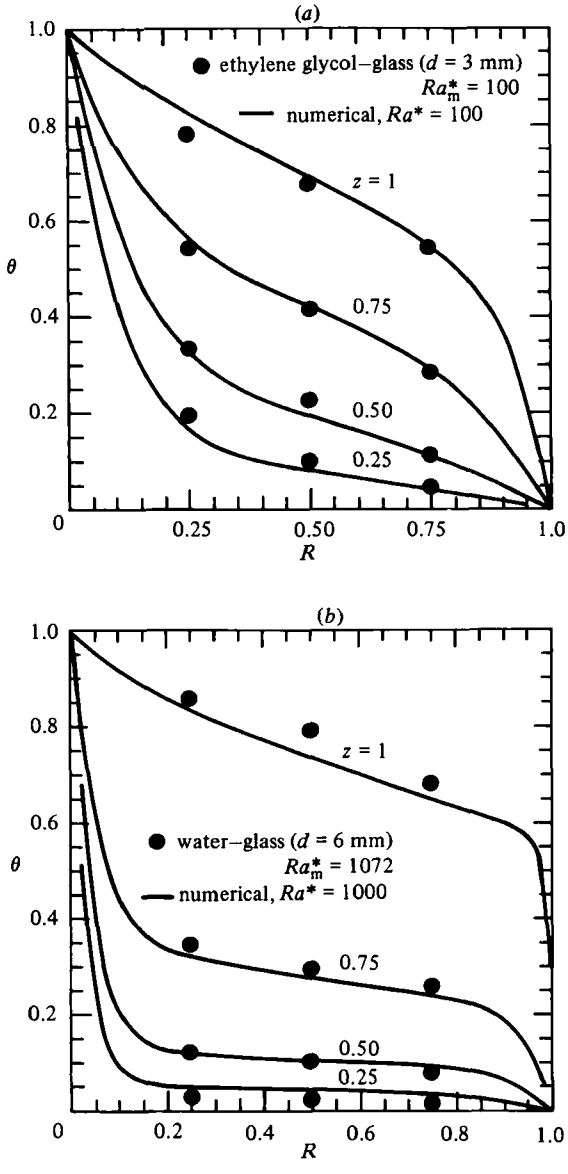

FIGURE 2. For caption see facing page.

consistent with what has been concluded in (*a*) for the upper region, but does not seem to agree with the temperature behaviour in the lower region.

To examine further the local behaviour of temperature for various media, the temperature distribution with respect to Grashof number $Gr^* = g\beta KD\,\Delta T/\nu^2$ may be considered. Temperatures for $Gr^* \simeq 175$, 467 and 880 are presented in figures 5(*a–c*) for the square annulus. As can be observed, the temperatures for water–steel are in general higher than those for water–glass, when $Z \leqslant 0.75$, for any fixed value of Gr^*. At $Z = 1$ the water–steel temperatures are initially higher ($Gr^* \approx 175$, figure 5*a*), but start dropping as the strength of convective flow increases. Finally, at $Gr^* \approx 567$ (figure 5*b*) they are lower than the local temperatures for water–glass, and continue to decrease further as Gr^* increases (figure 5*c*). The behaviour of the temperature

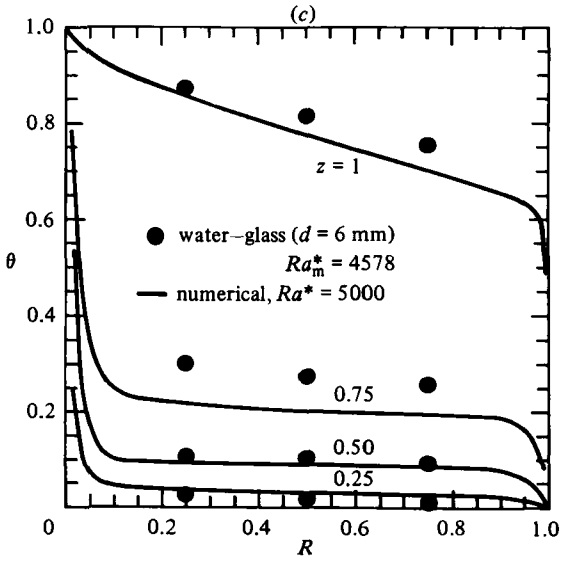

FIGURE 2. Temperature distribution for $A = 1.46$ and $\kappa = 5.338$: (*a*) $Ra^* \approx 100$; (*b*) 1000; (*c*) 5000.

distributions for heptane–glass with respect to those for water–glass is the same as what has been discussed in the earlier paragraphs.

The overall conclusion is that a lower value of k_f/k_s reduces temperature for any point in a lower region of the annulus ($Z < 0.75$ in the present case). This 'lower region' appears to depend on the geometry and Grashof, or Rayleigh, number. As $Z \rightarrow 1$ this behaviour is reversed, and, finally, temperatures for the lowest value of k_f/k_s are largest at $Z = 1$. In the case where $k_s \gg k_f$ much stronger convective flows are required for this behaviour to persist.

It may be noted that some of the same conclusions and observations on temperature distributions can be drawn from the data presented by Seki *et al.* (1978) for a vertical cavity with $A = 10$. Their temperature profiles clearly indicate that, at the centre of the cavity, θ increases as the Rayleigh number is increased. This increase is a maximum for the case of an oil–glass medium in comparison with water–glass and ethanol–iron media. Clearly, these temperatures are higher than the theoretical predictions.

Optically measured temperature fields reported by Klarsfeld (1970) for vertical cavities also substantiate our observations. Measured temperatures at the cavity centre obtained by Klarsfeld are generally larger than the theoretical values. For $Ra^*_m = 324.5$ and $A = 2.25$, $T(0.5, 0.5)$ is 19 °C instead of 18.5 °C (theoretical) for a temperature difference of 5° across the gap.

4.2. *Heat-transfer results*

In this subsection we begin the presentation of heat-transfer results for the vertical porous annulus that will proceed from the primary relations between the Nusselt and Rayleigh numbers to an extended discussion of the previously described divergent characteristics of data that appear in the literature for both vertical cavities and horizontal layers. In a sense, the problem of representing the Nusselt-number–Rayleigh-numbers relation universally has been anticipated by the behaviour of the

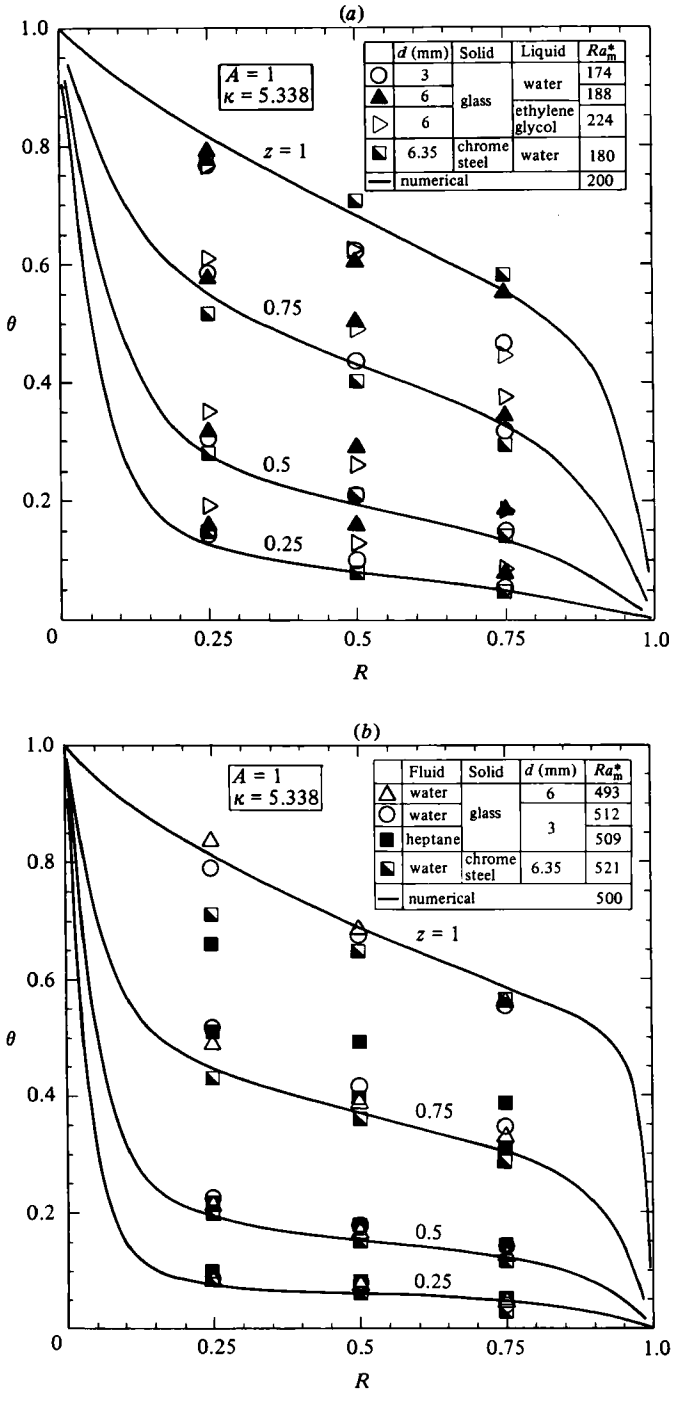

FIGURE 3. For caption see facing page.

temperature distributions with different fluid–solid media, or equivalently, different values of k_f/k_s. Generally, the heat-transfer data are presented in this subsection in the form

$$Nu_m = \text{constant} \times Ra_m^{*r} \tag{9}$$

for each aspect ratio.

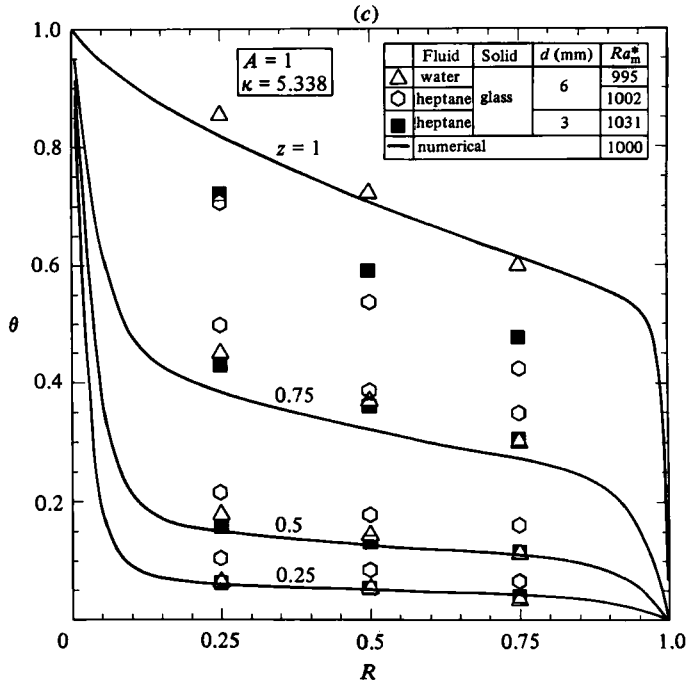

FIGURE 3. Temperature distribution for a square annulus: (*a*) $Ra^* \approx 200$; (*b*) 500; (*c*) 1000. Temperatures for water–glass are reproduced from Prasad and Kulacki (1984*b*).

For $A = 1.46$ Nusselt numbers for $10 < Ra^*_m < 5000$ with water–glass ($d = 6$ mm) and glycol–glass ($d = 3$ mm) are presented in figure 6 along with the results obtained by a finite-difference analysis (Prasad & Kulacki 1984*a*). In the conduction regime the experimental values of Nu_m agree well with numerical results, but in the asymptotic flow regime the experimental data fall below the theoretical values. The maximum difference is about 25%. With an increase in Ra^*_m, this difference diminishes, to about 6% for $Ra^*_m > 450$.

One of the reasons for the experimental values being lower may be the conduction losses through the top and bottom plates, and hence the absence of perfectly insulated horizontal boundaries. Though these losses have been properly accounted for in calculating Nu_m from experimental data, the boundary conditions for the top and bottom walls for the experiments are not exactly the same as assumed in the numerical analysis. As has been reported by Raithby & Wong (1981), for air-filled vertical cavities, a linear temperature distribution on the horizontal boundary results in lower values of average Nusselt number as compared with a true zero heat flux boundary. The difference between the Nusselt numbers for these two boundary conditions increases as the aspect ratio is reduced, and is reported to be maximum at $A = 1$. As the Rayleigh number is increased the temperature distribution on the upper boundary approaches that for a perfectly insulated surface (see figures 3*a–d*). Hence the relative effects of conduction through the top plate diminish, and a better agreement between the experimental and numerical results is obtained.

In the boundary-layer regime the correlation based on the experimental results is obtained as

$$Nu_m = 0.627\,Ra^{*0.517}_m, \quad Ra^*_m > 300, \quad A = 1.46, \tag{10}$$

whereas the numerical values are correlated by

$$Nu = 0.577\,Ra^{*0.521}, \quad Ra^* > 200, \quad A = 1.46. \tag{11}$$

The experimental data show a maximum deviation from (10) of 3.3%.

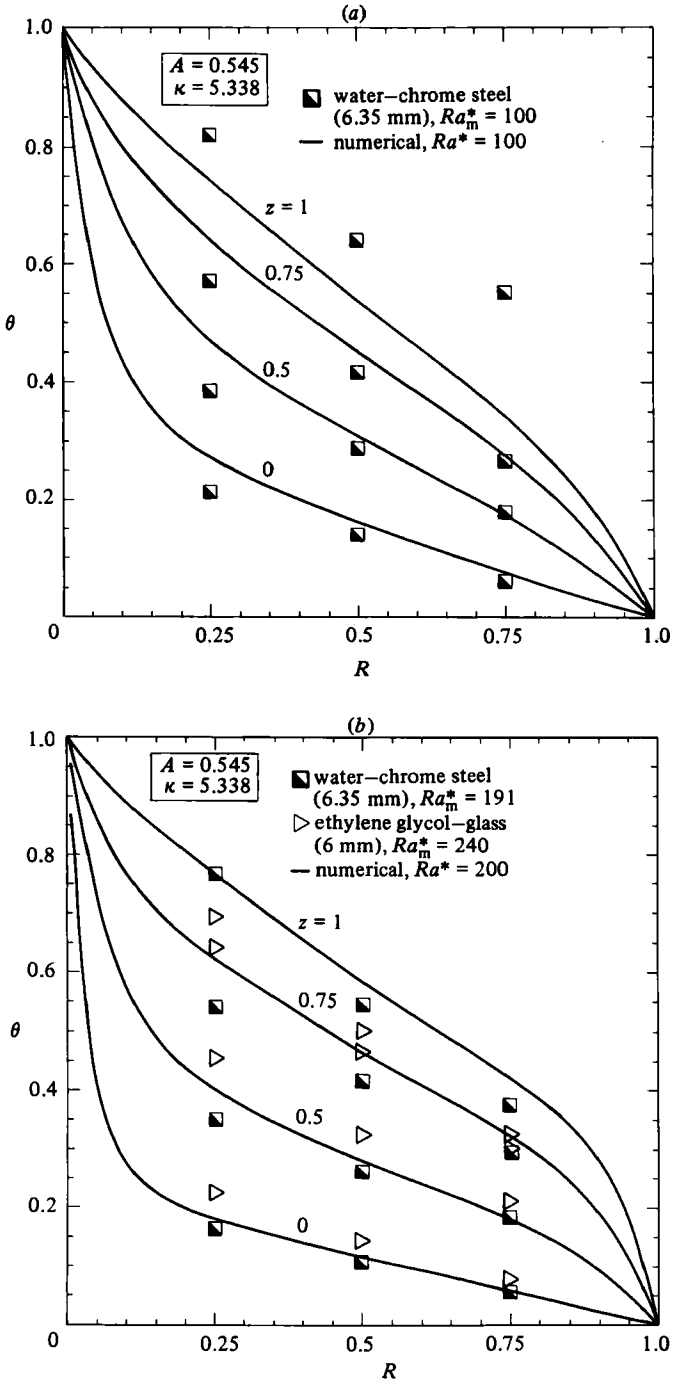

FIGURE 4. For caption see facing page.

For $A = 1$ (figure 7) a similar agreement is observed between the numerical and experimental values of Nusselt number for water–glass experiments (Prasad & Kulacki 1984*b*). Heat-transfer rates obtained for other porous media such as heptane–glass, water–steel and glycol–glass do not show such good agreement with the theoretical predictions. When compared with the results of water–glass experi-

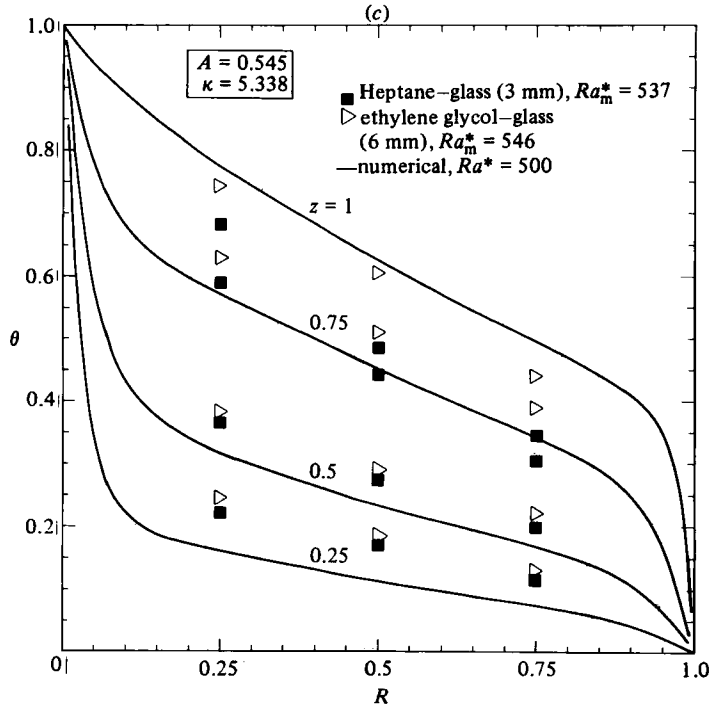

FIGURE 4. Temperature distribution for $A = 0.545$ and $\kappa = 5.338$: (*a*) $Ra^* \approx 100$; (*b*) 200; (*c*) 500.

ments it is observed that the Nusselt number for all other solid–fluid combinations are lower than that for water–glass. This difference between the Nusselt numbers for water–glass and any other medium grows as the Rayleigh number increases. For example, for $Ra_m^* \approx 300$, Nu_m for heptane–glass is within 2% of that for water–glass, whereas at $Ra_m^* > 3000$ the difference between the two values is more than 25%. Similarly, at very low Ra_m^*, water–steel results are very close to water–glass results, but, at $Ra_m^* \approx 520$, the difference between the two values are about 35%.

In figure 7 the Nusselt numbers for glycol–glass are observed to lie in between the water–glass and water–steel or water–glass and heptane–glass results in the corresponding ranges of Rayleigh number. This is contrary to what has been reported by Seki *et al.* (1978). Based on their experimental results for vertical cavity, they have concluded that Prandtl number of medium, Pr_m^*, has a strong effect on the heat-transfer rate. They have obtained an exponent of 0.13 for Pr_m^* when they correlated their data. In the present experiments, Pr_m^* for glycol–glass varies between 100 and 40, whereas for water–glass $3 \leqslant Pr_m^* \leqslant 5$. Hence the lower values of Nu_m for a medium having a large Prandtl number compared with that for water–glass does not support the above conclusion of Seki *et al.* (1978).

Another interesting aspect of the results is the change in the slope of curve drawn through the points for any particular medium, e.g. for heptane–glass or water-steel. It can be observed that the rate of increase in Nusselt number decreases with an increase in Rayleigh number; that is, the slope of such a curve decreases as Ra_m^* increases.

To characterize this behaviour, a set of experiments was conducted with 22.25 mm diameter glass balls. The heat-transfer rates for these large glass balls with water are always lower than that for small glass beads, for the present range of Rayleigh

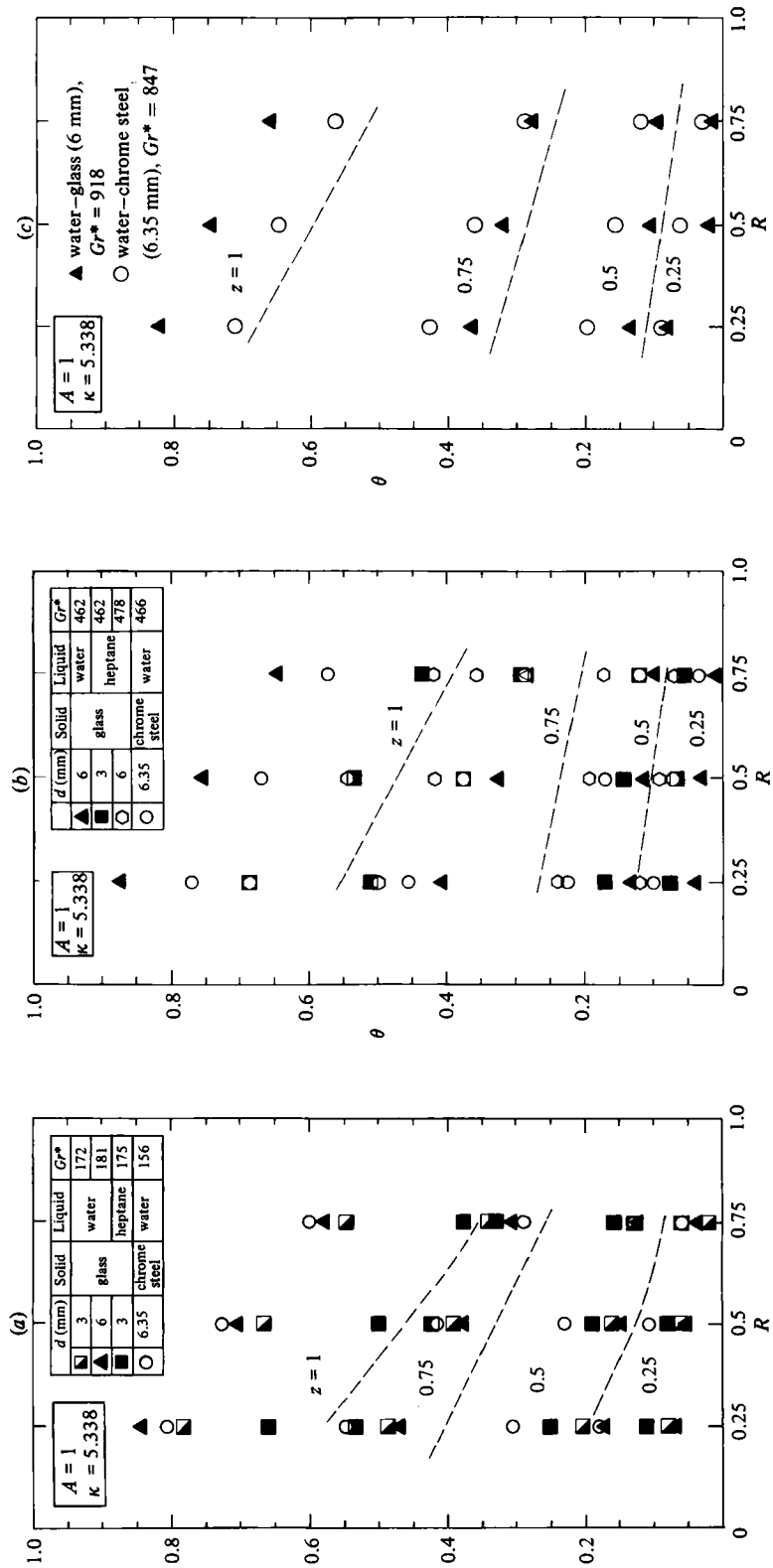

FIGURE 5. Recorded temperatures for $A = 1$ and $\kappa = 5.338$: (*a*) $Gr^* \approx 171$; (*b*) 467; (*c*) 883.

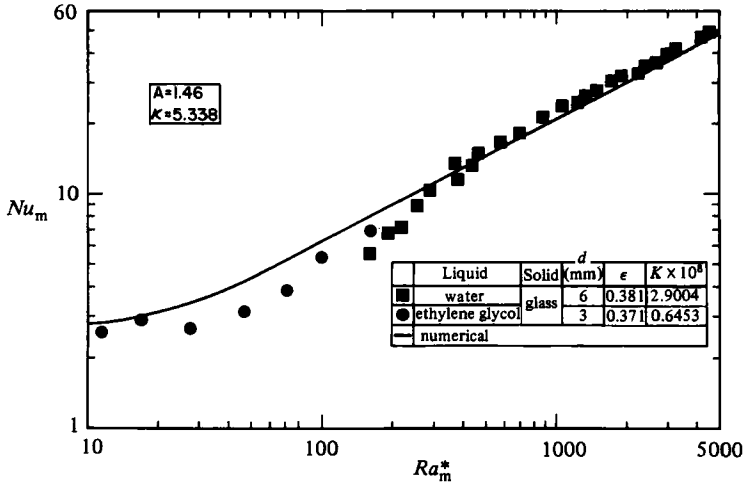

FIGURE 6. Heat-transfer results based on stagnant thermal conductivity for $A = 1.46$ and $\kappa = 5.338$.

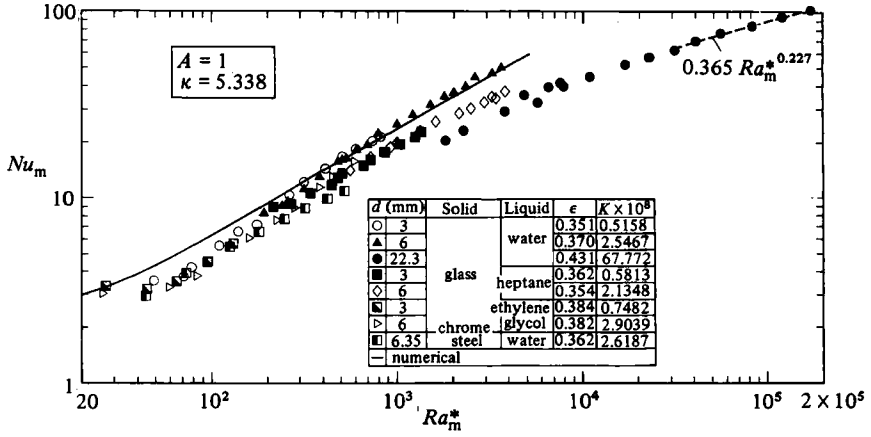

FIGURE 7. Variation in Nusselt number based on stagnant thermal conductivity, for various solid–fluid combinations, and $A = 1$. Water–glass results for 3 and 6 mm beads are taken from Prasad & Kulacki (1984*b*).

number, $Ra_m^* > 2000$. The slope of the curve for 22.25 mm diameter glass balls diminishes very fast as Ra_m^* increases, and at high Rayleigh numbers the experimental values of Nusselt number can be correlated by

$$Nu_m = 0.365 Ra_m^{*0.277}, \quad Ra_m^* > 3.5 \times 10^4, \quad A = 1. \tag{12}$$

The change in exponent for Ra_m^* from a value close to 0.5 to 0.277 is significant. It may be noted that the exponent for Ra_t, in the case of liquid-filled cavities and annuli, is reported to lie between 0.25 and 0.3 for laminar flow (Thomas & Vahl Davis 1970; McGregor & Emery 1969; Prasad & Kulacki 1984*c*).

Heat-transfer results for $A = 0.545$ and $\kappa = 5.338$ are presented in figure 8. The behaviour of the Nusselt number with respect to the Rayleigh number and several solid–fluid combinations is very similar to what has been observed for the square annulus. In the present case the slope of the curve for any particular medium changes much faster with increases in Rayleigh number as compared with that for $A = 1$. Even

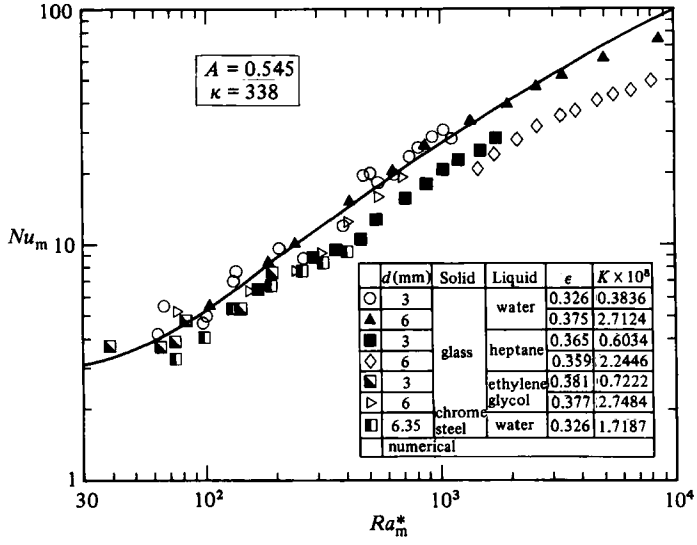

FIGURE 8. Variation in Nusselt number Nu_m, for various solid–fluid combinations, $A = 0.545$.

for the water–glass medium, the experimental values of Nu_m are lower than the numerical predictions when $Ra_m^* > 2000$. The slope of the curve for 6 mm glass beads and water is close to 0.4 for $Ra_m^* > 5000$. Furthermore, the heat-transfer rates for 6 mm beads are lower than that for 3 mm beads, which is clearly indicated by the heptane–glass data for the two sizes of beads in the overlapping range of Ra_m^*. This is in spite of the fact that Pr_m^* for 3 mm beads is lower than that for 6 mm beads in that range of Rayleigh number. In the case of $A = 1$, no such variation in Nusselt numbers for 3 and 6 mm beads is observed, though the heat-transfer results for 22.25 mm glass balls are quite a bit lower.

It is thus apparent that the Nusselt number is not only a function of solid–fluid combinations, but also depends on the diameter of the solid beads. The effect of the bead size is mostly reflected in the permeability, but the present results for $A = 1$ and 0.545 indicate that the size of the enclosure is also a factor in relation between the Nusselt and Rayleigh numbers. This has been demonstrated by the agreement of water–glass ($d = 6$ mm) results with the numerical predictions for $A = 1$ and variation in two results for $A = 0.545$ for the reported range of Ra_m^*. Also, it should be mentioned that the divergence of results for various fluid–solid combinations cannot be attributed to the improper selection of values for the stagnant thermal conductivity. An inspection of figures 6–8 confirms this point. At low Rayleigh numbers, close to the conduction regime the overlapping data for various fluid–solid combinations are in good agreement. It is only at higher Rayleigh numbers, where the convective heat transfer becomes dominant, that the results begin to diverge.

4.3. *Discussion of present results*

The divergence in present heat-transfer results is very similar to that reported by various investigators. Though several models have been proposed so far, to explain the large-scale divergence in heat-transfer rates, as discussed in §1, none of them provide a satisfactory answer to the problem. The non-validity of infinite heat-transfer coefficient h between the solid and fluid (Combarnous & Bories 1974) may be reasonable, but the theoretical model based on a suitable value of heat-transfer coefficient between the solid particles and the fluid is quite complex and is not able

to provide satisfactory results to match the experimental values. The effect of Prandtl number as reported by Seki *et al.* (1978) does not seem to be acceptable in the light of present results for high Prandtl number. To find an answer to the problem, the present experimental results for $A = 1$ will be looked at in various ways.

In figure 9 the present heat-transfer results are presented in terms of fluid Rayleigh and Nusselt numbers. The implication is that the presence of solid particles is ignored. These Nusselt numbers are then compared with Nu_f for a water-filled annulus (Prasad & Kulacki 1984*c*). As can be seen, the results for 22.25 mm glass balls and water are initially lower than that for pure water, but the difference diminishes as the Rayleigh number increases. For $Ra_f > 5 \times 10^8$ the Nusselt numbers are within 5 % of each other. The last five points for glass–water are correlated by

$$Nu_f = 0.353 Ra_f^{0.261}, \quad Ra_f > 10^9, \tag{13a}$$

where $Ra_f = g\beta D^3 \Delta T/\nu\alpha_f$, and $Nu_f = \bar{h}D/k_f$. The exponent of the Rayleigh number is quite close to that obtained for fluid-filled vertical cavity and annulus. In fact, the correlation for a water-filled annulus of the same aspect and radius ratios is (Prasad & Kulacki 1984*c*)

$$Nu_f = 0.305 Ra_f^{0.271}. \tag{13b}$$

Hence the implication is that a very small fraction of energy is transferred in the present case, by conduction through the solid glass beads, which seems to be reasonable for a highly permeable porous medium near the wall. This situation can also be characterized by saying that the loss in convective heat transfer due to the presence of the solid matrix is compensated by the conduction through them.

Figure 9 also contains the results for 6 mm diameter glass beads with water and heptane. As can be seen, not only does the slope of the curve for the water–glass ($d = 6$ mm) medium change very rapidly with increasing Ra_f, but the values of Nu_f for the heptane–glass medium are also very close to that for the water–glass data in the overlapping range of Rayleigh number. Furthermore, the heptane–glass data follow nearly the same trend with Ra_f as the water–glass data. Even though the Prandtl number of heptane is comparable to that of water, the conductivity of water is about 4.5 times greater than that of heptane. Hence the glass should account for a large conduction contribution to the heptane–glass medium. In the overlapping range of Rayleigh number this larger conduction contribution of glass beads in the case of the heptane–glass medium should therefore result in higher values of Nu_f compared to those for the water–glass medium, which is not the case. It is thus concluded that conduction heat transfer through the solid, as a percentage of overall heat transfer, decreases very rapidly as the Rayleigh number increases. This rate of decrease depends on the permeability of medium, particularly near the wall.

To illuminate further the effect of the Prandtl number, consider figure 10, where the Nusselt number is plotted against the Grashof number for $A = 1$. The water–glass data ($3 < Pr_m^* < 5$) are all higher than the heptane–glass points ($1.7 < Pr_m^* < 2$), which in turn are higher than the water–steel points ($0.5 < Pr_m^* < 0.9$). This clearly indicates that, the larger the Prandtl number, the higher is the heat-transfer rate for a given Gr^*. Even the Nusselt numbers for only water–glass (or heptane–glass) media with two different sizes of beads support this conclusion if we ignore the unknown effects of the change in porosity and permeability. (The Prandtl number for 6 mm diameter beads is lower than that for 3 mm diameter beads for a fixed Gr^* owing to the difference in mean temperatures of the two media.) The question is whether or not this Prandtl-number effect can be expressed by having the same exponents for Gr^* and Pr_m^*, such that in (6) $s = 0$ and only r needs to be considered.

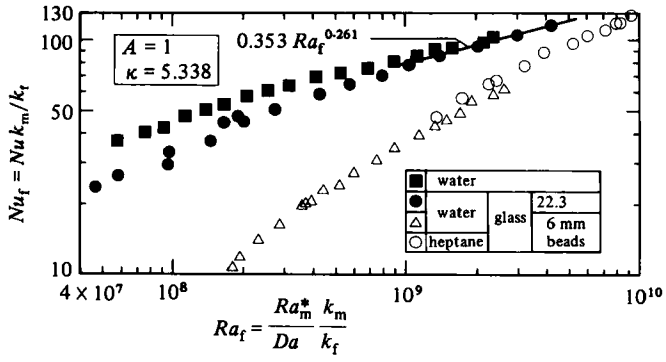

FIGURE 9. Present experimental results for $A = 1$, in terms of fluid Rayleigh and Nusselt numbers and compared with pure-water results, obtained from Prasad & Kulacki (1984*c*).

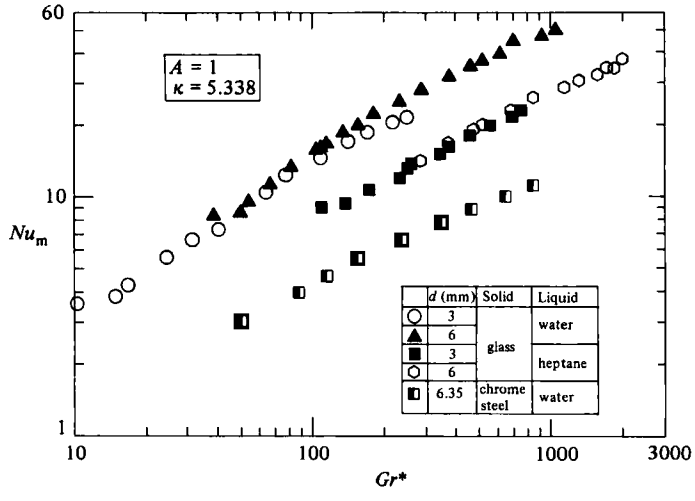

FIGURE 10. Nusselt number based on stagnant thermal conductivity, Nu_m for water–glass, $3 < Pr_m^* < 5$; heptane–glass, $1.7 < Pr_m^* < 2$; and water–steel, $0.5 < Pr_m^* < 0.9$.

Generally, Prandtl-number effects on free convection in fluid-filled rectangular cavities has been found to be quite small when heat-transfer results are presented in the form

$$Nu_f = \text{constant} \times Ra_f^m\, Pr_f^n\, A^p, \tag{14}$$

and it can be expected that heat transfer in a porous cavity should be similarly influenced, at least at high Rayleigh numbers. A recent study by Graebel (1981) on the influence of the Prandtl number on free convection in a rectangular cavity indicates that the Nusselt number increases by 1.5% when the Prandtl number is varied from unity to infinity for a given Rayleigh number. McGregor & Emery (1969) have reported a correlation for the heat transfer in the same geometry and have obtained $n = 0.012$. In the case of the vertical annulus, Kubair & Simha (1982) have obtained a *negative* value of $n = -0.07$, which is based on their experimental and numerical work for $0.02 < Pr_f < 6$. A recent study by Keyhani & Kulacki (1984) on free convection in a tall vertical annulus with air, helium and water as the working fluids supports the above conclusion. On the other hand, the early numerical work of Thomas & de Vahl Davis (1970) for a vertical annulus ($1 \leqslant A \leqslant 33$) gives a weak dependence with $n = 0.006$, and an experimental study of Prasad & Kulacki (1984*c*) reports $n = 0.017$ for $A = 1$ and $4 < Pr < 196$. Thus the kind of differences in the

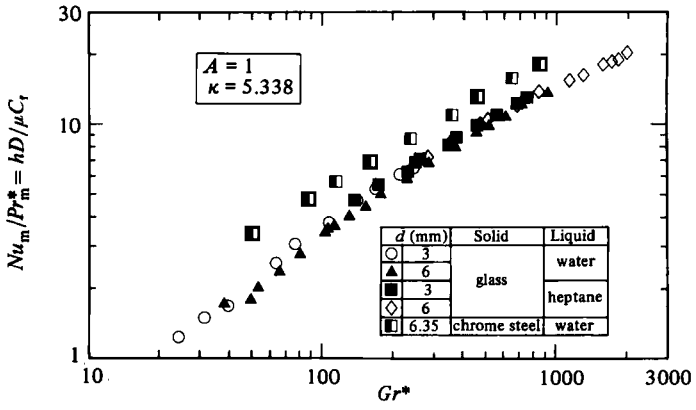

FIGURE 11. Variation in Nu_m/Pr_m^* (a parameter independent of thermal conductivity) with Grashof number.

Nusselt numbers seen in figures 7 and 8 are most likely a result of the parameters chosen, and a physically correct analysis of the experimental data should universally represent the effect of the medium on the relation between the Nusselt and Rayleigh numbers.

Another way to look at the present results is to plot the data in terms of parameters that do not involve the thermal conductivity of the medium. This has been done in figure 11 where Nu_m/Pr_m $(= hD/\mu C)$ is plotted versus Gr^*. Here the data for the water–steel medium ($0.5 < Pr_m^* < 0.9$) give the highest values of Nu_m/Pr_m^*. However, Nu_m/Pr_m^* for a heptane–glass medium ($1.7 < Pr_m^* < 2$) are not higher than those for a water–glass ($3 < Pr_m^* < 5$). The implication is that the water–glass and heptane–glass media must have the same effective Prandtl number. As discussed previously, the use of k_m in the calculation of the Prandtl number is acceptable for low Rayleigh numbers where the convective heat transfer is not dominant (see figure 7). However, once convective heat transfer becomes dominant, the effective thermal conductivity of the medium becomes a function of the flow parameters as well. Also, the fraction of energy transport by the fluid increases as Gr^* increases, and the effective thermal conductivity of the medium should be expected to change and tend towards the fluid conductivity. For the present data the result would be a reduction in the value of effective thermal conductivity k_e, much more for heptane–glass than for water–glass. This would then lead to the enhancement in Nusselt and Prandtl numbers for both media, but by different proportions, such that, at high Grashof number ($Gr^* > 300$), Nu_e and Pr_e^* are almost the same for both media. In the case of water–steel the change in k_e with Gr^* would bring the water–steel results closer to those for water–glass.

As is evident from the above discussion, the effective thermal conductivity k_e would never change if k_s and k_f were the same. Consequently, media with such fluid–solid combinations yield heat-transfer data generally in close agreement with analytical and numerical predictions. The close agreement of the experimental data of various investigators obtained for a water–glass medium with analytical and numerical predictions confirms this.

4.4. *A model for effective thermal conductivity*

From the preceding, it is now proposed that a simple weighting procedure be adopted to account for the flow-dependence of the effective thermal conductivity. At any Rayleigh number, the fraction of heat transferred by convection is given by

$$w = 1 - \frac{\text{heat transfer by conduction}}{\text{total heat transfer}}. \tag{15}$$

Here 'convection' is used to mean that component of heat transfer due to fluid flow apart from the conductive amount due to the mean temperature gradient. For the present case of an annulus,

$$w = 1 - \frac{k_m}{r_i \bar{h} \ln (r_o/r_i)}, \tag{16}$$

where $\bar{h}$ applies to the inner wall of the annulus. Generally, (15) may also be written as

$$w = 1 - \frac{Nu_{cond}}{Nu_m}. \tag{17}$$

The effective thermal conductivity is then given by

$$k_e = wk_f + (1-w)\, k_m, \tag{18}$$

where w depends on geometric parameters and convective state in the porous medium.

Reformulation of the present data

The present experimental results for various aspect ratios have been reformulated in terms of (16) and (18) and are presented in figures 12–14. In figure 12 Nusselt numbers Nu_e are plotted versus Rayleigh numbers Ra_e^*, for $A = 1$ and $\kappa = 5.338$. A marked difference in the behaviour of the data (compare with figure 7) for the several fluid–solid combinations is seen. Not only have the experimental data been brought together, with the single exception of the Nusselt numbers for the 22.25 mm diameter glass balls, but they are in good agreement with the numerical results as well. The scatter in the measured Nusselt numbers has been reduced to $\pm 6\,\%$, and a correlation can be obtained in the form

$$Nu_e = 0.394 Ra_e^{*0.610}, \quad Ra_e^* > 300, \quad A = 1, \tag{19}$$

whereas the numerical values are correlated by

$$Nu_e = 0.485 Ra_e^{*0.564}, \quad 200 < Ra_e^* \leqslant 5000, \quad A = 1. \tag{20}$$

For the present set of results ($A = 1$), the thermal conductivity for water–glass (k_e versus k_m) reduces by a maximum of 18 %, whereas that for heptane–glass and water–steel decreases by about 66 % at the highest Rayleigh numbers reported here. Correspondingly, the Rayleigh and Nusselt numbers also change. The effect on the Prandtl number is in the same proportion, and Pr_e^* for heptane–glass, water–steel and glycol–glass approach that for the water–glass, as Ra_e^* increases. At $Ra_e^* \approx 4000$, the Prandtl numbers for heptane–glass and water–glass differ by only 20 %.

The above agreement between the numerical and experimental results for various porous media is not fortuitous. In the energy equation (3), k is not the stagnant thermal conductivity, but the conductivity of the medium when the fluid is flowing. Hence the Rayleigh number obtained from the non-dimensionalization of the momentum equation is based on the effective thermal conductivity k_e, not the stagnant conductivity k_m as is conventionally done. Consequently, the Nusselt number that one obtains by solving the system of partial differential equations analytically or numerically is also based on k_e. This puts a restriction on the use of analytical or numerical results for design purposes because the value of k_e is not known beforehand. This difficulty can be easily overcome, and the value of k_e for a given Rayleigh number Ra_m^* can be obtained from available information. This will be discussed further in §4.5.

While it is true that the Nusselt numbers for the 22.25 mm diameter balls diverge significantly from the apparent relation between the Nusselt and Rayleigh numbers

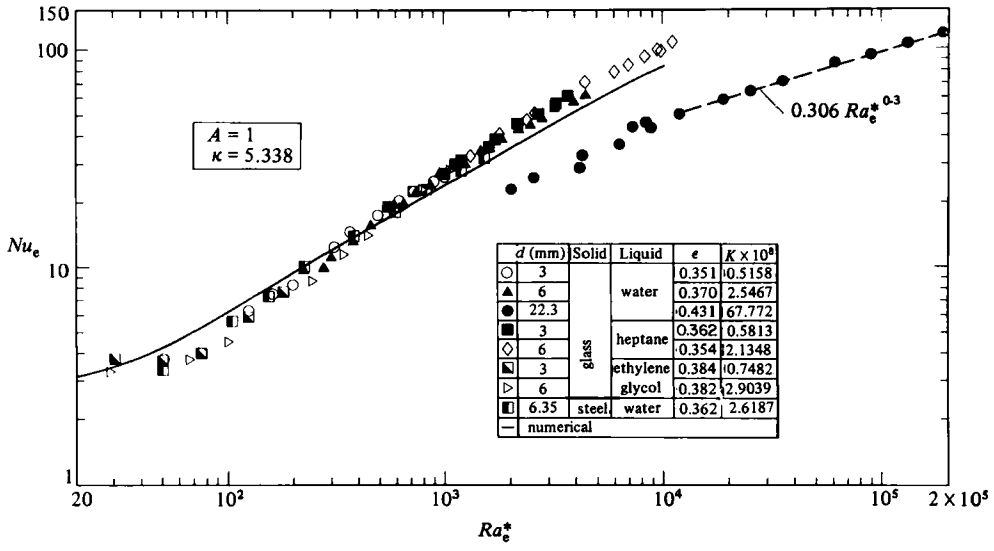

FIGURE 12. Nusselt number based on effective thermal conductivity, Nu_e, for various solid–fluid combinations, $A = 1$.

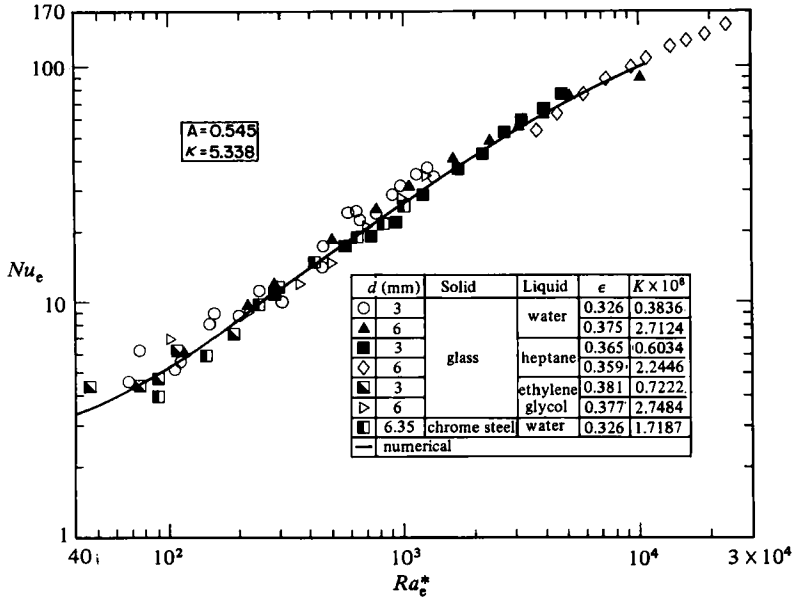

FIGURE 13. Nusselt number based on effective thermal conductivity Nu_e, for $A = 0.545$.

in figure 12, we believe this is a result of a failure of Darcy's law. In the experiments from which these data were taken, the number of balls which could fit across the annulus was between five and six. Thus, near both walls of the annulus, permeability was quite high and was strongly dependent on location along and normal to the wall. From these data, we propose that, for a given medium, there is a combination of D/d *and* Ra_e^* for which Darcian behaviour does not exist, and the assumptions used in the volume-averaged form of the conservation equations do not hold. We will return to this point in §4.6.

A similar collapse of the experimental data for $A = 0.545$ and 1.46 around the

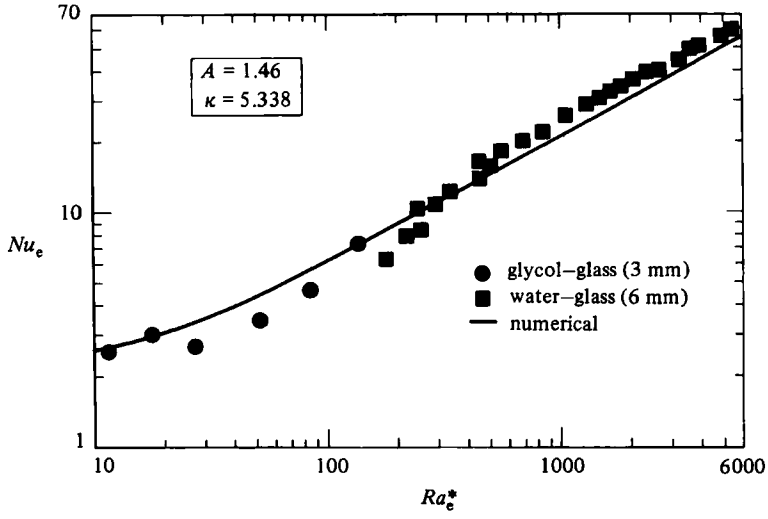

FIGURE 14. Modified experimental results for $A = 1.46$.

numerical predictions is seen in figures 13 and 14. In figure 13 the scatter is greatest for the water–glass medium ($d = 3$ mm). This set of experiments was done under various temperature and power conditions to test the repeatability of the experimental data (Prasad 1983). However, for both aspect ratios, the agreement between the data and the numerical predictions is considered reasonable.

Reformulation of previous results

To show further the effectiveness and applicability of the proposed model for the effective thermal conductivity, the experimental results of Schneider (1963), Combarnous (1970) and Buretta & Berman (1976) for vertical and horizontal porous layers are presented in figures 15–17. Schneider's results have been modified by obtaining the Nusselt and Rayleigh numbers from the graphs given in his paper and values of k_f/k_m quoted there. Combarnous's and Buretta & Bermans' data have been directly taken from the dissertations of Combarnous (1970*a*) and Buretta (1972).

For Schneider's results for the vertical rectangular cavity, the Nusselt numbers for water–glass and turpentine–glass now agree within a reasonable accuracy (figure 15). The Nusselt number for turpentine–glass is within 4% of that for water–glass at $Ra_e^* \approx 2000$, whereas the original difference was 35% (Schneider 1963). The points for turpentine–steel are also very close to the Nu_e for other media when $d = 5$ mm. For $d = 15$ mm no such agreement is observed. It may be noted that the width D of the layer for Schneider's experiments was only 40 mm, giving $D/d = 2.67$. A dip in the trend of Nu_e versus Ra_e^* can also be seen for the 10 mm diameter glass beads with turpentine as the fluid for $Ra_e^* > 1000$. The value of D/d in this case is 4, and hence this deviation in the measured Nusselt numbers from the trend established at lower Rayleigh numbers takes place at a larger Ra_e^* than for the 15 mm diameter steel balls. This behaviour represents a delay in the departure from a Darcian system for the given fluid–solid combination, D/d and Rayleigh number. In figure 15 the agreement between the reformulated experimental results and the numerical predictions is considered reasonable and is greatly improved over that of the original plot in terms of Nu_m and Ra_m^* given by Schneider (1963).

The experimental results of Combarnous (1970*a*, *b*) are presented in figure 16 along with the analytical results of Gupta & Joseph (1972). Compared with the original plot

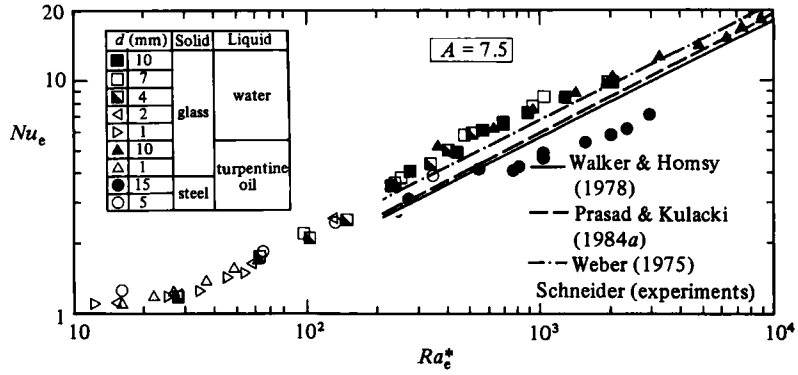

FIGURE 15. Schneider's experimental data (modified) for vertical rectangular cavities compared with theoretical results.

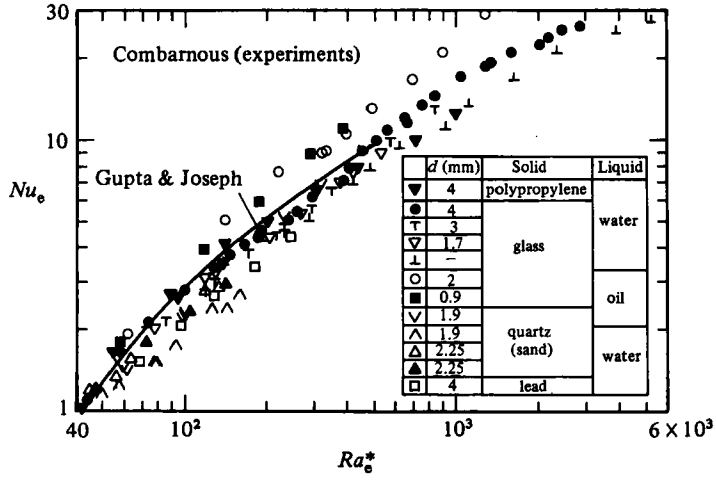

FIGURE 16. Modified experimental results of Combarnous (1970) for horizontal porous layers and analytical results of Gupta & Joseph (1973).

given by Combarnous, a much closer agreement is seen for all of his data for the several fluid–solid combinations considered, except for oil as the fluid. A most interesting aspect of the reformulated results is the absence of a definite trend in the data for a particular combination of fluid and solid. However, the degree of scatter is greatly reduced, with Nusselt numbers falling within a reasonable band about the prediction of Gupta & Joseph. With respect to the data for oil as the fluid, Nusselt numbers are invariably higher than those for water. A similar observation can also be made from the results of Seki *et al.* (1978) for a vertical porous cavity. The behaviour of the data for oil is probably very much affected by a temperature-dependent high viscosity, and thus an inappropriate use of Ra_e^* as a single independent parameter for correlation purposes. For temperature-dependent high-viscosity fluid, one would need to consider those parameters arising out of additional viscous terms as proposed by Brinkman (1949) and others.

Schneider's results for the horizontal layer are presented in figure 17 with the experimental results of Buretta & Berman (1976) and the analytical results of Gupta & Joseph (1973). As in the case of Combarnous's data, a similar improvement is obtained when the Nusselt and Rayleigh numbers are reformulated in terms of k_e.

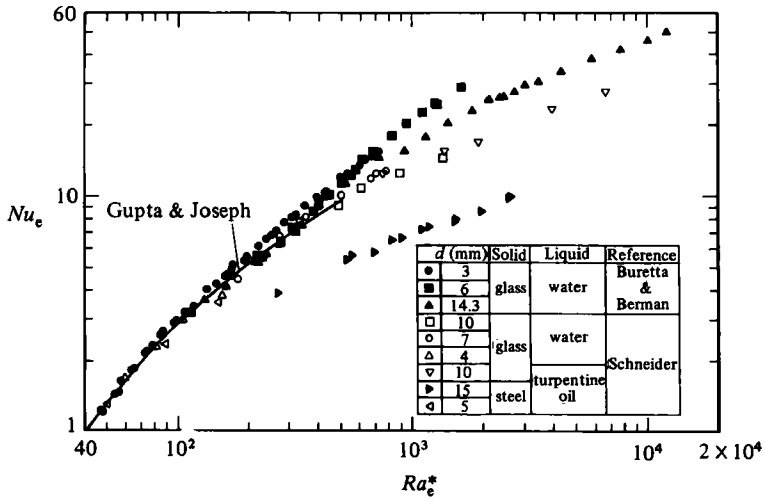

FIGURE 17. Modified experimental results of Schneider (1963) and Buretta & Berman (1976) for horizontal layers.

(It is interesting to compare figure 17 with figure 37 presented by Cheng (1978) for the same data.) As in the previous case, there is a deviation of the data from the trend established at low values of Ra_e^* for the larger-diameter beads, but in figure 17 the agreement between the data from both experimental studies, as well as the analytical results, is considered quite good for $Ra_e^* < 1000$. A similar improvement in the agreement between the water–glass and water–steel data is observed for the recent experiments of Catton (1984).

4.5. *Calculation procedure for* k_e

It is possible to obtain the corrected value of k_e and then the proper values of the Rayleigh and Nusselt numbers by using the heat-transfer results based on the above mathematical formulation (§1). This, of course, implies a semiempirical and, generally, *ad hoc* procedure, but at this point we can propose no other method owing to the way in which the governing differential equations are usually formulated and the absence of a precise method for determining the percentages of energy transferred by the solid and the fluid as a function of Rayleigh number. Fortunately, a simple procedure, as outlined below, can be followed with good results.

First, one finds the Rayleigh number $Ra_m^{*(1)}$ based on the lengthscale appropriate to the geometry at hand. This value of $Ra_m^{*(1)}$ determines $Nu_m^{(1)}$ from the established relation between the Nusselt and Rayleigh numbers. Equations (15)–(18) are then used to obtain $w^{(1)}$ and $k_e^{(1)}$ respectively. Values of $Ra_e^{*(1)}$ and $Nu_e^{(1)}$ can then be calculated, and this redefines either the experimental data or numerically predicted (Ra_e^*, Nu_e)-pair for the given Rayleigh number. With the first iteration, new values of w and k_e can be calculated to compute improved (Ra_e^*, Nu_e)-pairs. When the value of the nth iteration for effective thermal conductivity has converged to the desired level, the procedure is terminated and the final values of the Rayleigh and Nusselt numbers are taken as the corrected data. Either experimental data based on k_e or theoretically predicted heat-transfer results can be used as the basis for this procedure.

Table 2 presents corrected Rayleigh and Nusselt numbers for $A = 1$ and $\kappa = 5.338$ for several fluid–solid combinations. For all aspect ratios of the present study, the

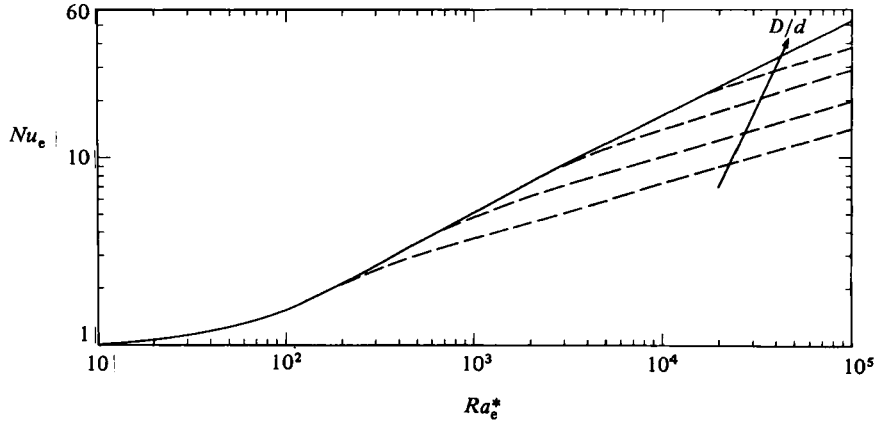

FIGURE 18. Proposed parametrization of heat-transfer data when branch curves appear at high Rayleigh numbers. Branch points indicate breakdown of Darcian flow assumption.

			Based on experimental data		Based on numerical results	
Medium	Ra_m^*	Nu_m	Ra_e^*	Nu_e	Ra_e^*	Nu_e
water–glass	262.4	10.43	309.4	12.30	309.5	12.30
	511.9	16.97	615.1	20.40	612.2	20.30
	994.9	22.17	1208.4	30.47	1203.7	30.35
	3582.0	50.10	4370.9	61.13	4363.2	61.03
heptane–glass	446.0	11.86	983.2	26.14	950.4	25.26
	857.6	17.93	2171.4	45.39	2051.4	42.89
	1327.1	22.82	3532.3	60.75	3348.7	57.59
	3807.9	37.21	11073.0	108.20	10753.2	105.07
ethylene	170.5	6.07	241.1	8.59	255.4	9.10
glycol–glass	278.8	8.90	437.6	13.98	443.8	14.17
	589.0	15.97	1033.6	28.03	1010.5	27.40
water–chrome	180.4	6.58	378.3	13.80	378.3	13.80
steel	318.7	8.86	818.1	22.74	787.6	21.89
	521.3	10.94	1526.2	32.03	1472.8	30.91

TABLE 2. Comparison of modified Rayleigh and Nusselt numbers obtained by using experimental data and numerical results, for $A = 1$, $\kappa = 5.338$

agreement between corrected Nusselt numbers based on the experimental data and those based on the numerical analysis is quite good. For $A = 1$ and 0.545 the agreement is to within 5–6%, and this level of uncertainty is well within the range of the precision of both the experiments and numerical analysis.

4.6. *Breakdown of Darcian flow*

The foregoing has pointed to several factors which appear to have a substantial influence on the Nusselt number but have not been explicitly identified and related in previous studies. These are k_f/k_s, k_m, k_e and D/d. Additionally, divergence of the Nusselt-number–Rayleigh-number curve from trends established at low Rayleigh numbers cannot be completely eliminated by the use of the effective thermal conductivity k_e. Generally, the change in the heat-transfer relation is marked by a well-defined change in the slope when ln Nu_e is plotted versus ln Ra_e^* and apparently signals the end of Darcian behaviour for that particular system. After such a change

in slope, the Nusselt numbers do not follow predicted values obtained via numerical analysis under the usual volume-averaging rules and assumptions underlying Darcy's law. In this section we propose a way to view the data to account in part for a breakdown of Darcian flow.

From an analysis of our data, and, to some extent, that of others, we propose that for any solid–fluid combination the ratio D/d is the parameter that best characterizes the change in the slope of the Nusselt-number–Rayleigh-number relation and allows one to parametrize a particular branch for a given system (a cavity filled with porous media). Further, the tendency of these branch curves must be toward the relation between the Nusselt and Rayleigh number for a fluid-filled cavity. Although we cannot demonstrate this here with either conclusive experimental data or numerical analysis, we offer the following argument.

First it is necessary to consider figure 17, wherein the Nusselt numbers for the 15 mm diameter balls diverge sooner ($Ra_e^* \approx 200$ at the point of divergence) than those for the 14.3 mm diameter glass balls ($Ra_e^* \approx 1000$ at the point of divergence). The corresponding values of D/d are 2.67 and 6.16 (Schneider 1963; Buretta & Berman 1976). Even the data for 10 mm diameter balls diverge earlier than that for 14.3 mm diameter balls since D/d is lower in the former case (4 versus 6.16). Data for the present study for an annulus with $A = 1, \kappa = 5.338$ (figure 12) shows a branch curve for 22.25 mm diameter balls in a water–glass system that appears to diverge somewhere between $Ra_e^* = 200$ and 900. Similar behaviour is demonstrated by the results of Schneider and Seki *et al.* (figure 15) for a vertical cavity. For each of these branch curves, the slope starts decreasing as soon as it branches out from the main curve (theoretical prediction) and approaches that for the fluid-filled cavity. For the present results (figure 12) the slope of the Nusselt-number–Rayleigh-number curve is 0.3 when $Ra_e^* \geqslant 2.5 \times 10^4$. The slope of Buretta & Bermans' data for the 14.3 mm diameter balls (figure 17) is close to 0.35 when $Ra_e^* > 5000$, whereas Schneider's data for the large steel balls ($d = 14.3$ mm) show a slope close to 0.3. These values are reassuring in view of existing literature for a fluid-filled cavity. For such a cavity the Nusselt number may be expressed as

$$Nu_f = C' Ra_f^m, \tag{21}$$

where C' is a constant and the subscript f denotes properties for the fluid alone. For the laminar boundary-layer flow in vertical annuli and the rectangular cavities, the predicted value of m lies between 0.25 and 0.33 (Sheriff 1966; Thomas & de Vahl Davis 1970; Prasad & Kulacki 1984*c*; McGregor & Emery 1979; also recall (13*b*)).

At the point where Darcian behaviour breaks down, the effects of flow channelling near the wall may be the most important factor that initiates a fundamental change in the Nusselt-number–Rayleigh-number relation (Vafai & Tien 1981). As the Rayleigh number is increased for a given fluid–solid combination, the boundary layer near the wall reaches a thickness where it is of the order of the ball diameter. This implies that the porosity and permeability in the boundary layer are very much higher and the volume-averaged conservation equations are no longer valid. Hence the quantity δ/d, where δ is the local boundary-layer thickness, would be the correct parameter for the wall-channelling effects. For an enclosure, such as a vertical annulus or rectangular cavity, $\delta \propto D$, and the parameter D/d emerges as the parameter that designates where certain branches of the Nusselt-number–Rayleigh-number curve start.

If this idea is extended to a consideration of very high Rayleigh number, a given Nusselt-number–Rayleigh-number curve should become parallel to that for the

fluid-filled cavity of the same dimensions, i.e. regardless of the value of D/d, the end result is an appropriate branch curve. This is not seen when experimental data are reported at low Ra_m^* (Reda 1983) or when D/d is extremely large, e.g. when fine sand or ground-glass particles are used as the porous matrix.

Generally, when a branch is reached in a particular system, the Nusselt-number–Rayleigh-number relation can be represented as

$$Nu_e = C'' Ra_f^m, \tag{22}$$

where m will take on the same values as in (21), and C'' depends on the Darcy number Da and k_f/k_e since $Ra_e^* = Ra_f Dak_f/k_e$. For a given system the Darcy number is a constant and k_f/k_e would be close to unity at high Ra_e^*. It is speculated that, in the case of a shallow cavity, the ratio L/d of cavity length to particle size may be another parameter that influences the breakdown of Darcian flow behaviour, whereas for an annulus r_i/d may also need to be considered.

5. Conclusion

Heat-transfer results obtained from the experiments with a vertical annulus filled with various saturated porous media show that there is reasonably good agreement with numerically predicted Nusselt numbers for glass–water media when experimental Rayleigh and Nusselt numbers are presented in the conventional way, i.e. based on the stagnant thermal conductivity k_m. The agreement is not very good when either the particle diameter relative to the characteristic length of the enclosure is very high or the Rayleigh number is too large. Nusselt numbers for all other fluid–solid combinations diverge, i.e. exhibit a non-unique relation between the Nusselt and Rayleigh numbers. The higher the Rayleigh number or the larger the deviation of k_f/k_s from unity, the greater is the divergence in the Nusselt number. A similar divergence of the heat-transfer data for vertical and horizontal rectangular cavities has been reported in the literature by several investigators as well.

By analysing the present experimental data in various ways, it is shown that this divergence is not due to an explicit effect of Prandtl number as suggested by some of the previous investigators. Further consideration of the present data has led to the conclusion that the major cause of this large-scale divergence is the use of an improper thermal conductivity for the porous medium. Based on the fact that the fraction of energy transported by the fluid flow increases as the Rayleigh number is increased, a simple model for an effective thermal conductivity k_e is proposed. The model takes into account the enhanced effect of fluid thermal conductivity as a function of convective flow. Use of this value of conductivity for the porous medium not only eliminates the variation among the Nusselt numbers for various media, but also brings them very close to the theoretical predictions over wide ranges of Rayleigh numbers and fluid–solid combinations. Similar improvements are observed in the experimental results of previous investigators for horizontal layers or vertical cavities.

Although, in the present case or for previous experimental studies, the effective thermal conductivity is obtained by using the experimental data directly, an iterative scheme is also presented for the estimation of k_e by using the established theoretical relation between Nusselt and Rayleigh numbers. Excellent agreement is achieved between the two values of k_e.

From the success of using the effective thermal conductivity, we propose that there exists a unique relation between the Nusselt and Rayleigh numbers unless the

conditions that assure the validity of Darcy's law are violated. The experimental data illustrate this in the branching behaviour that appears at certain Rayleigh numbers for given fluid–solid combinations when the Rayleigh number is large enough. It is argued physically that this is a result of flow-channelling effects near solid boundaries when the boundary layer reaches the order of the mean particle (or pore) size. For the tall cavity, the dimensionless group that parametrizes such branches in the Nusselt-number–Rayleigh-number relation is the ratio D/d of cavity width to the particle size. The smaller the value of D/d, the lower the value of Ra_e^* at which branching will occur. From the present experiments and an analysis of previous experimental data, it is proposed that the slope for branch relation between Nu_e and Ra_e^* approaches that for a fluid-filled enclosure of the same geometry when the Rayleigh number is large enough. Generally, at very low Rayleigh numbers none of these characteristics are encountered because boundary layers are large relative to particle (or pore) size, or the entire enclosure is dominated by viscous flow and a low component of convective heat transport.

In view of the recent emphasis on the use of porous media produced by using solid particles for various engineering applications, the characterization of branch points and branch relations is of practical value. The conditions under which the slope of the branch curve for Nu_e versus Ra_e^* approaches that for the fluid-filled enclosure also needs to be understood. It may be interesting to study the effects of a few other parameters, e.g. L/d for a shallow rectangular cavity or r_i/d for an annular enclosure, on this branching behaviour. Further experiments are required to accomplish this.

REFERENCES

Bear, J. 1972 *Dynamics of Fluids in Porous Media*. Elsevier.

Bories, S. A. & Combarnous, M. A. 1973 *J. Fluid Mech.* **57**, 63.

Brinkman, H. C. 1949 *Appl. Sci. Res. Suppl.* **2–4**, 190.

Buretta, R. J. 1972 Thermal convection in a fluid filled porous layer with uniform internal heat sources. Ph.D. dissertation, Department of Aeronautical Engineering, University of Minnesota.

Buretta, R. J. & Berman, A. S. 1976 *Trans. ASME* E: *J. Appl. Mech.* **48**, 249.

Catton, I. 1984 In *Proc. NATO Advanced Study Institute on Natural Convection: Fundamentals and Applications*. (Ed. W. Aung, S. Kakac & R. Viskanta). Hemisphere.

Chan, B. K. C., Ivey, C. M. & Barry, J. M. 1970 *Trans. ASME* C: *J. Heat Transfer* **2**, 21.

Cheng, P. 1978 *Adv. Heat Transfer* **14**, 1.

Combarnous, M. 1970*a* Convection naturelle et convection mixte en milieu poreux. Ph.D. thesis, University of Paris.

Combarnous, M. 1970*b* *Rev. Gen. Therm.* **9**, 1355.

Combarnous, M. 1972 *C.R. Acad. Sci., Paris* A **275**, 1375.

Combarnous, M. & Bories, S. A. 1974 *Intl J. Heat Mass Transfer* **17**, 505.

Combarnous, M. & Bories, S. A. 1975 *Adv. Hydrosci.* **10**, 231.

Elder, J. W. 1967 *J. Fluid Mech.* **27**, 29.

Graebel, W. P. 1981 *Intl J. Heat Mass Transfer* **24**, 125.

Gupta, V. P. & Joseph, D. D. 1973 *J. Fluid Mech.* **64**, 51.

Havstad, M. A. & Burns, P. J. 1982 *Intl J. Heat Mass Transfer* **11**, 1755.

Hickox, C. E. & Gartling, D. K. 1982 *ASME Paper* 82-HT-68.

Horton, C. W. & Rogers, F. T. 1945 *J. Appl. Phys.* **16**, 360.

Kaneko, T., Mohtadi, M. F. & Aziz, K. 1974 *Intl J. Heat Mass Transfer* **17**, 485.

Katto, Y. & Masuoka, T. 1967 *Intl J. Heat Mass Transfer* **10**, 297.

KEYHANI, M. & KULACKI, F. A. 1984 In preparation.

KLARSFELD, S. 1970 *Rev. Gen. Therm.* **9**, 1403.

KUBAIR, V. G. & SIMHA, C. R. V. 1982 *Intl J. Heat Mass Transfer* **25**, 399.

KULKARNI, A. V. 1983 Experimental studies on convective heat transfer in a vertical porous annulus with constant heat flux on the inner wall. M.S. thesis, Department of Mechanical and Aerospace Engineering, University of Delaware.

KUNII, D. & SMITH, J. M. 1960 *AIChE J.* **49**, 71.

LAPWOOD, E. R. 1948 *Proc. Camb. Phil. Soc.* **44**, 508.

MCGREGOR, R. K. & EMERY, A. F. 1969 *Trans. ASME* C: *J. Heat Transfer* **91**, 391.

PRASAD, V. 1983 Natural convection in porous media–an experimental and numerical study for vertical annular and rectangular enclosures. Ph.D. dissertation, Department of Mechanical and Aerospace Engineering, University of Delaware.

PRASAD, V. & KULACKI, F. A. 1982 *Heat Transfer in Porous Media.* ASME HTD, vol. 22, p. 35. [Also *Trans. ASME* C: *J. Heat Transfer* **106** (1984), 152.]

PRASAD, V. & KULACKI, F. A. 1983 *ASME Paper* 83-HT-66. [Also *Trans. ASME* C: *J. Heat Transfer* **106** (1984), 158.]

PRASAD, V. & KULACKI, F. A. 1984*a* *Intl J. Heat Mass Transfer* **27**, 207.

PRASAD, V. & KULACKI, F. A. 1984*b* *Trans. ASME* C: *J. Heat Transfer* (in Press). [Also *ASME Paper* 84-HT-76, *22nd ASME/AIChE Natl Heat Transfer Conf., Niagara Falls, 1984.*]

PRASAD, V. & KULACKI, F. A. 1984*c* Submitted to *Trans. ASME* C: *J. Heat Transfer.*

RAITHBY, G. D. & WONG, H. H. 1981 *Num. Heat Transfer* **4**, 447.

REDA, D. C. 1983 *Trans. ASME* C: *J. Heat Transfer* **105**, 795.

SEKI, N., FUKUSAKO, S. & INABA, H. 1978 *Intl J. Heat Mass Transfer* **21**, 985.

SCHNEIDER, K. J. 1963 In *Proc. 11th Intl Congr. on Refr.*, vol. II-4, p. 247. Pergamon.

SHERIFF, N. 1966 In *Proc. 3rd Intl Heat Transfer Conf.*, vol. 2, p. 132.

THOMAS, R. W. & DE VAHL DAVIS, G. 1970 In *Proc. 4th Intl Heat Transfer Conf.*, vol. 4, NC 24, Elsevier.

VAFAI, K. & TIEN, C. L. 1981 *Intl J. Heat Mass Transfer* **24**, 195.

WALKER, K. L. & HOMSY, G. M. 1978 *J. Fluid Mech.* **97**, 449.

WEBER, J. E. 1975 *Intl J. Heat Mass Transfer* **18**, 569.

WOODING, R. A. 1957 *J. Fluid Mech.* **2**, 273.

YAGI, S., KUNII, D. & WAKAO, N. 1961 In *Intl Developments Heat Transfer*, p. 742. ASME.

YEN, Y. C. 1974 *Intl J. Heat Mass Transfer* **17**, 1349.